Pultrusion Manufacturing and Flexural Behavior Analysis of Thermoplastic Polymer-based FRP Composites for High-strength Applications

C. Mackin and G. Saha*
Nanocomposites and Mechanics Lab, Department of Mechanical Engineering, University of New Brunswick, Fredericton, NB, E3B 5A3, Canada
* Gobinda Saha (gsaha@unb.ca)

ABSTRACT

High-flexural-strength composite materials are desired in many applications: heat-absorbing tiles in defence/satellites/under water vehicles, 3D smart antenna, hydro-turbine blades, submarine hulls, thermal/ballistic/shock-resistant materials, etc. Fiber-reinforced polymer (FRP) composites when designed/developed with thermoplastic polymer can accommodate 3-5 times larger failure strain and a similar vibration damping coefficient by replacing conventional thermosetting polymers. This paper presents research results obtained from pultrusion manufacturing of 9.3-mm-diameter thermoplastic GFRP rebars. Microstructural analysis of the novel composites was performed using 3D optical profilometry. The composite flexural properties were assessed in a 3-point-bend test. Results indicate that good bonding between the fibre and the thermoplastic polymer was accomplished, in addition to proving that thermoplastic GFRP rods can obtain similar flexural characteristics to their thermosetting counterparts.

KEYWORDS: Thermoplastic polymer composite; Flexural properties; High-strength applications

1 INTRODUCTION

This paper will discuss the outcomes of a thermoplastic pultrusion process for manufacturing glass fiber reinforced polymer (GFRP) rods. In pultrusion manufacturing, the two most common polymer types used are thermosets and thermoplastics.

In a typical thermosetting pultrusion setup, glass or carbon fibers pass through a resin bath where dry roving's are soaked in resin at atmospheric pressure and temperature. The wetted fibers then pass through a set of guide plates before entering a heated die. The glass-matrix product is then cured in the die while being pulled through via a set of pulleys at the exit. Upon exiting the heated die, the rods are completely solid.

Thermosetting polymer resins have been the standard in large-scale industrial manufacturing and research for pultrusion processes as described above, since thermosetting resins generally have a thin viscosity which allows the fibers to become sufficiently saturated with resin. Thermoplastic resins are generally much more viscous than the thermosetting variety, making them a non-ideal solution for impregnation-based pultrusion, and therefore there has been less research in this area.

In addition to viscosity, there are a number of differences between thermosets and thermoplastics. From a chemistry standpoint, thermosets solidify via a cross-linking reaction in the polymer matrix (Baran, 2015). Thermoplastics, on the other hand, cure with the formation of molecular chains which are connected via hydrogen bonding. Thermoplastics are reformable, in that their shape can be modified after the polymerization process has occurred, under the appropriate thermal and pressure loading. Thermoplastics are also recyclable, meaning that under the required heat conditions, the polymer resin can be separated from the glass, and both GFRP components can be recycled separately. It is also reported that thermoplastic pultruded products have greater impact strength when compared to their thermosetting counterparts.

These advantages over existing solutions make thermoplastics an attractive resin for pultrusion manufacturing. For the first time, a poly methyl-methacrylate-based (PMMA) thermoplastic resin is being tested to develop a novel pultrusion process to produce thermoplastic GFRP rods to gain knowledge of the flexural properties in pultruded rebars.

2 METHODS USED AND PROCESS

The thermoplastic pultrusion process designed uses the same equipment used in a thermosetting process. For typical thermoplastic processes, however, a cooling section/die is commonly installed to allow the pultruded product to solidify completely. When the manufactured rods, in this case, exit the heated die after curing, they are still in a semi-solid state; that is, their shape is still slightly malleable to the touch and if not enough cooling time is allowed, the pulleys driving the pultrusion process may distort the structure of the final product. As mentioned previously, thermoplastic FRPs are reformable, and therefore when the rods exit the heated die, it is as though the rod is still in its reformable state; a cooling section allows the pultruded product adequate cooling time to avoid reformation.

2.1 Process

The goal of the process designed is to produce solid GFRP rods, which can be used in rebar applications. The process begins with dry, continuous glass fiber rovings passing through a resin bath, after which the wetted fibers pass through a series of guide plates until the wetted product is in the shape of a rod. This non-polymerized product then enters a heated die, which is 90 cm in length. The die is heated from the top and the bottom using electric strip heaters, and the temperature is adjusted via PID controllers that take input from a series of T type thermocouples which are inserted into the midsection of the die. While the resin and fiber is passing through the heated die, pulleys at the end of the process are pulling the product. These pulleys feature a circular hole passthrough such that the shape of the rods is retained as much as possible. The pulleys are controlled via a dial and switch system which allows the pulling speed to be adapted or turned off on the fly in case of manufacturing defects or emergency. Upon exiting the heated die, the rods were cooled with convective heat transfer via a hand-held hair dryer on a cool setting, acting as the cooling section for this pultrusion process. Finally, the solid rods are manually cut to their desired length. This setup is shown in Figures 1 and 2 below.

Figure 1: Side view of pultrusion set-up

Figure 2: Top view of pultrusion set-up

2.2 Recipes Developed

It is common for filler products to be used in pultrusion manufacturing to add value to the final product (Rothon, 2017). Fillers have the potential to add strength, flame resistance, UV and impact resistance, as well as reducing costs since less resin is required to fill the matrix surrounding the fibers.

To determine if fillers have a place in thermoplastic processes, pultruded GFRP rods were produced using aluminum oxide as a filler at 20% and 30% by weight, as well as kaolin (obtained from Composites One, Montreal, QC) at 20% by weight. Each of the rods produced contained the same percentage of glass fiber, estimated to be 76.5%. Two control rods were also produced, one using the PMMA-based thermoplastic, and the other using a vinyl ester-based thermosetting resin, for a total of 5 rods under investigation.

All thermoplastic experiments used the same chemical percentages, meaning the same percentages of resin, lubricant, initiators, and glass were used to determine the difference between the various fillers and percentages used. The thermosetting rods also used the same glass fibers, however, the chemistry, heating, and pulling setup was adjusted for the vinyl ester-based polymer composition. These recipes are outlined in Table 1 below.

Table 1: Recipes developed for analysis

Title	Resin	Initiators	Additives	Heater	Pulling Speed
Al_2O_3 - 30%	Thermoplastic PMMA	• tert-butyl peroxybenzonate • Norox 500-75OMS • Perkadox 16	Aluminum Oxide @ 30% by weight	Heater #1: 110ºC Heater #2: 110ºC Heater #3: 110ºC	0.15m/min
Al_2O_3 - 20%	Thermoplastic PMMA	• tert-butyl peroxybenzonate • Norox 500-75OMS • Perkadox 16	Aluminum Oxide @ 20% by weight	Heater #1: 110ºC Heater #2: 110ºC Heater #3: 110ºC	0.15m/min
Kaolin - 20%	Thermoplastic PMMA	• tert-butyl peroxybenzonate • Norox 500-75OMS • Perkadox 16	Kaolin @ 20% by weight	Heater #1: 110ºC Heater #2: 110ºC Heater #3: 110ºC	0.15m/min
Thermoplastic	Thermoplastic PMMA	• tert-butyl peroxybenzonate • Norox 500-75OMS • Perkadox 16	None	Heater #1: 110ºC Heater #2: 110ºC Heater #3: 110ºC	0.15m/min
Thermoset	Thermosetting Vinyl Ester	• tert-butyl peroxybenzonate • Norox 500-75OMS • Norox PULCAT AMB	None	Heater #1: 120ºC Heater #2: 150ºC Heater #3: 150ºC	0.33m/min

2.3 Bending Testing

Once the pultruded rods were manufactured as described above, samples from these rods were taken to produce microstructure images of each cross-section. 3-point-bending test was conducted to determine the flexural properties of each resin-filler combination. The pultruded GFRP rods were cut to a length of 35 cm and placed within the supports of an Instron SATEC Model T10000 Materials Testing System, which was modified to support a 3-point-bending test setup as shown below in Figure 3. This system was controlled via the Instron Partner™ Materials Testing Software, which records deflection values in millimeters, force applied in Newtons, as well as the time in seconds at which each data point was collected. This data was saved as a .csv file for each rod tested, after which all datasets were imported into MATLAB where force-displacement and stress-strain curves were produced, as well as calculations for the Young's modulus and maximum force, stress, and deflection values for each rod.

Figure 3: Instron SATEC Model T10000 Materials Testing System

2.4 Calculations

For calculations, the ASTM D790 designation was followed, which is designed for determining the flexural characteristics of FRPs. The calculations used are outlined in formulas (1) and (2) below:

$$\sigma_f = \frac{FL}{\pi R^3} \tag{1}$$

$$\epsilon_f = \frac{6Dd}{L^2} \tag{2}$$

where σ_f is the flexural stress, ε_f is the flexural strain, F is the load applied in Newtons, L is the span between the two supports of the bending test in mm, D is the deflection measured in mm, d is the diameter of the circular rod tested in mm, and R is the radius of the rod in mm (ASTM International, 2017).

To determine the Young's modulus, the difference in stress was divided by the difference in strain when taking two data points from a straight-line path of the stress-strain curve. The averages of the Young's moduli, as well as maximum loads, displacements, and stress values were plotted on separate bar graphs for all 5 sample sets tested, including their respective standard deviations. All results calculated can be found in section 3.

3 RESULTS

Microstructural images were obtained using 3D optical profilometry. These images for each of the respected samples can be seen in Figures 4 to 8 below.

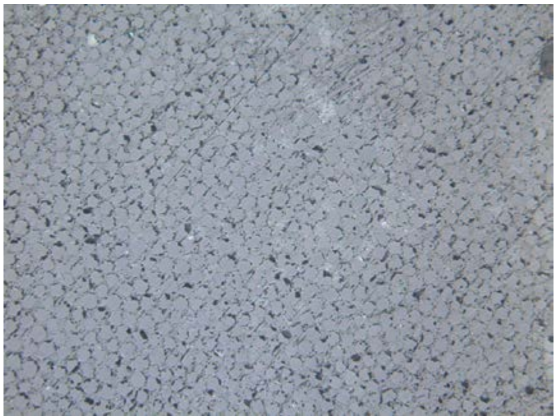

Figure 4: Al_2O_3 at 30%

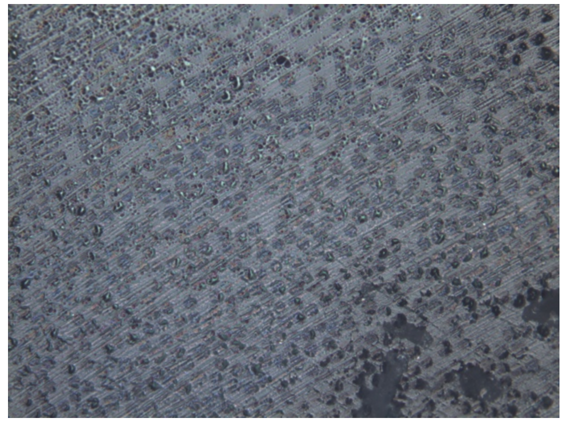

Figure 5: Al_2O_3 at 20%

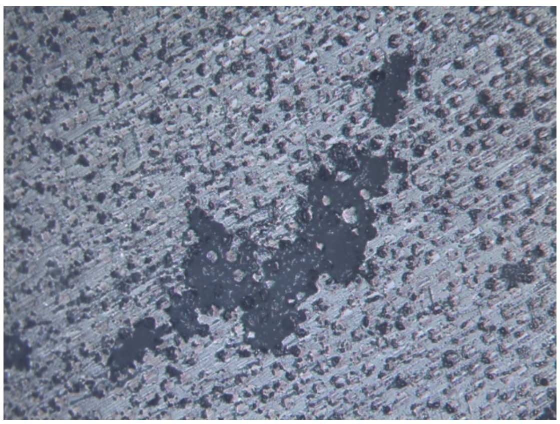

Figure 6: Kaolin at 20%

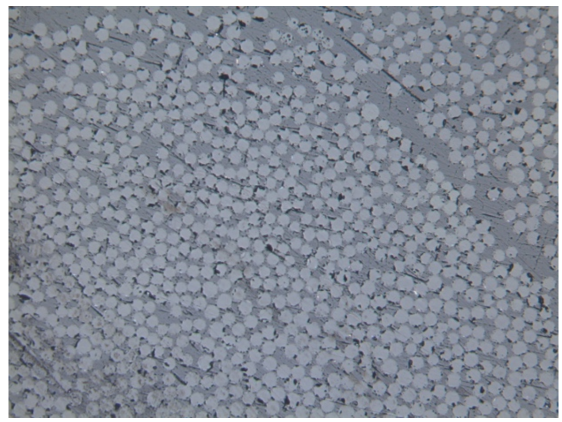

Figure 7: Thermoplastic control rod, no filler

Figure 8: Thermosetting control rod, no filler

The results gathered from the study described above include microstructure images of each of the samples tested, as well as the average range of the maximum stress, load, deflection, and Young's modulus values for all 5 of the rods produced. The results from each of these metric comparisons are outlined in their own respective bar graphs, which can be found in Figures 9 to 12 below. Each graph also includes the standard deviations for each sample analyzed.

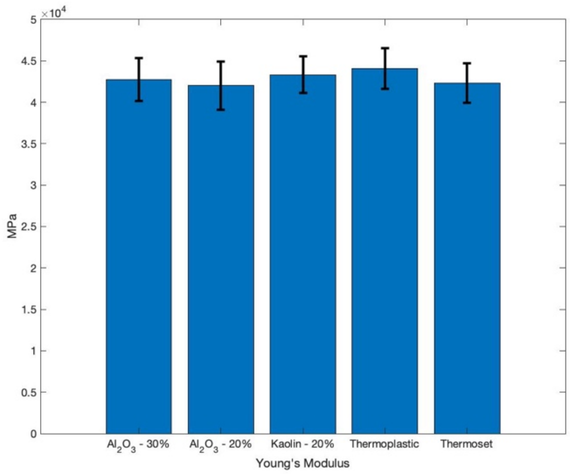

Figure 9: The average range of Young's modulus for all 5 experiments

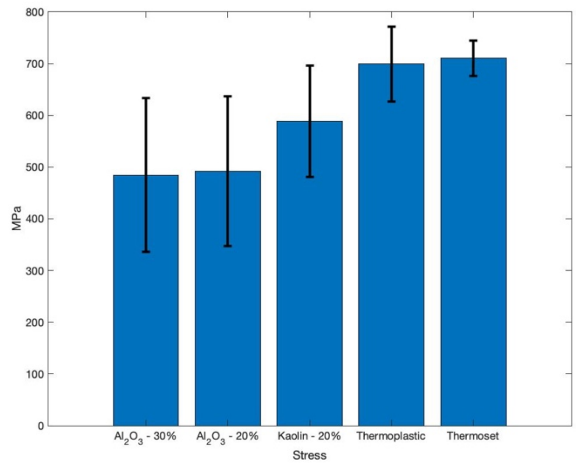

Figure 10: The average range of the maximum stress value for all 5 experiments

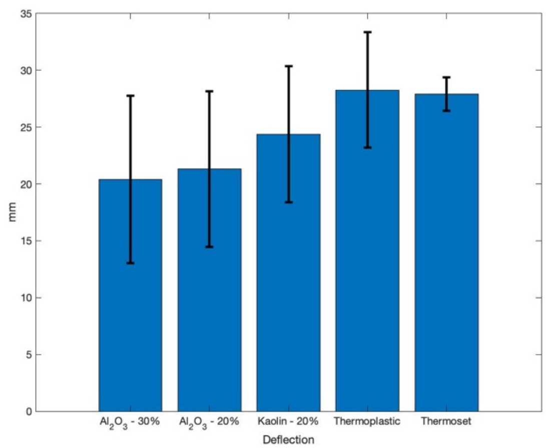

Figure 11: The average range of the maximum deflection value for all 5 experiments

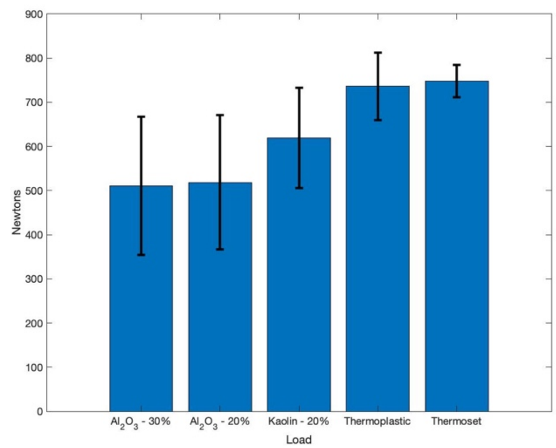

Figure 12: The average range of the maximum deflection value for all 5 experiments

These bar graphs are also summarized in Table 2 below, featuring the average values for each metric calculated.

Table 2: Average values of Young's modulus and maximum load, stress, and deflection, for all 5 samples

Title	E (MPa)	Load (N)	Stress (MPa)	Deflection (mm)
Al_2O_3 - 30%	42720.11	510.33	484.69	20.38
Al_2O_3 - 20%	42015.69	518.24	492.20	21.31
Kaolin - 20%	43324.61	619.66	588.52	24.36
Thermoplastic	44085.10	736.13	699.14	28.27
Thermoset	42312.12	747.84	710.26	27.92

4 DISCUSSION

The microstructure images produced exhibit good bonding between the glass fiber and the surrounding matrix. In some locations of the cross sections of both 20% filler cases, porosities exist which could mean there is not enough matrix product combining with the glass. Research in this regard is on-going to help determine an explanation for the existence of porosities in thermoplastic GFRP rebars.

When observing the differences in the 3-point-bending results, there are some clear differences. It was found that the thermoplastic control rods without fillers performed similarly to the thermosetting control rods, producing nearly identical values in all 4 metrics compared, as shown in Table 2 above. This is a promising result as it proves the use of a thermoplastic resin in pultrusion applications is possible, providing similar flexural characteristics to existing thermosets. For existing applications of thermoset GFRPs, thermoplastic components can be used instead to gain recyclability, reformability, and impact resistance.

For all 5 of the samples tested, the Young's modulus was found to be quite similar, regardless of the presence of a solid filler, ranging between 42.015 GPa and 44.085 GPa.

When a solid filler was combined with the thermoplastic resin, however, the pultruded rods did not perform as well as the control rods in maximum stress, loading, and deflection results. The rods containing aluminum oxide at 30% and 20% performed similarly, with the 20% concentration performing slightly better in deflection. Rods with kaolin at 20% performed better than the aluminum oxide rods in load, stress, and deflection cases. As shown in Table 2, kaolin allowed the rods to withstand an additional 100 N over the rods containing aluminum oxide.

The control rods performed the best, however, achieving the highest withstanding stress, load, and deflection of the samples analyzed. These rods were able to withstand more than an addition 100 N of load and 100MPa of stress over the kaolin rods. This result shows that aluminum oxide and kaolin in thermoplastic pultrusion of GFRP rods does not provide added flexural strength, but rather the contrary.

There are a number of explanations for this outcome. As mentioned previously, thermoplastics solidify by increasing the lengths of their polymer chains, whereas thermosets solidify via cross linking of the polymer chains. With added solid material in the surrounding matrix, these particles may be interfering with the resin, preventing the polymer chains from growing as long as they possibly can, thus reducing the strength of the GFRP rod. Instead of having strength with long polymer chains throughout the rod in the control setup, rods containing fillers may have more chains, but at a shorter length.

Another explanation for the decrease in flexural strength when using fillers stems from the microscopic structure of the fillers used. Due to the coarse microstructure present in aluminum oxide, it was found that the continuous glass rovings were cut by abrasion from the filler during the impregnation process. This resulted in an accumulation of glass shards at the entrance of the heated die, meaning the once continuous glass fibers now had discontinuities. It is expected that this defect would also affect the tensile strength of the GFRP rods. This issue was not present with the kaolin filler as it possesses a much smoother microstructure, which could explain why the kaolin rods performed better than the aluminum oxide rods.

5 CONCLUSIONS

This study was able to determine that the thermoplastic resin used in this pultrusion process performs similarly to existing thermosetting resins under flexural loads. For existing applications of thermoset GFRPs, thermoplastic components can be used instead to gain recyclability, reformability, and impact resistance. The results from this analysis also show that aluminum oxide and kaolin fillers do not offer improvements to flexural properties in thermoplastic GFRP rebars. The abrasive cutting of continuous fibers discovered proves that aluminum oxide can be problematic in pultrusion setups like the one shown in Figures 1 and 2.

In addition to the flexural and microstructure analysis described above, supplementary testing experiments will be conducted in the near future, including tensile strength, thermal loading, environmental corrosion, and flame resistance tests. With these analyses, the thermo-mechanical and environmental performance of thermoplastic GFRP rebars will be solidified.

6 ACKNOWLEDGEMENTS

This research would not have been possible without the knowledge and advice of my colleagues from the Nanocomposites and Mechanics Laboratory at UNB, including Chase Wallace and Xingzhi Jiang. The machining work done by Brian Guidry was integral to the project. Finally, the financial support from the Natural Sciences and Engineering Research Council Canada (NSERC-530673-18), and New Brunswick Innovation Foundation (NBIF STEM & Social Innovation Award) is greatly appreciated.

REFERENCES

Baran, I. (2015). Pultrusion: State-of-the-art process models, pp. 4.

Rothon, R. (2017). Fillers for Polymer Applications, pp. 1-7.

ASTM International. (2017). ASTM D790-17 Standard Test Methods for Flexural Properties of Unreinforced and Reinforced Plastics and Electrical Insulating Materials, retrieved from https://doi.org/10.1520/D0790-17.